

## Vortex-antivortex 'molecular crystals' in hybrid ferromagnet/superconductor structures

This article has been downloaded from IOPscience. Please scroll down to see the full text article.

2009 J. Phys.: Conf. Ser. 150 052019

(<http://iopscience.iop.org/1742-6596/150/5/052019>)

View [the table of contents for this issue](#), or go to the [journal homepage](#) for more

Download details:

IP Address: 146.175.13.243

The article was downloaded on 05/03/2013 at 11:12

Please note that [terms and conditions apply](#).

## Vortex-Antivortex ‘Molecular Crystals’ in Hybrid Ferromagnet/Superconductor Structures

S.J. Bending<sup>1</sup>, J.S. Neal<sup>1</sup>, M.V. Milošević<sup>1,2</sup>, A. Potenza<sup>3</sup>, L. San Emeterio<sup>3</sup> and C.H. Marrows<sup>3</sup>

<sup>1</sup>Department of Physics, University of Bath, Claverton Down, Bath, BA2 7AY, UK

<sup>2</sup>Departement Natuurkunde, Universiteit Antwerpen (UIA), B-2610 Antwerpen Belgium

<sup>3</sup>School of Physics and Astronomy, University of Leeds, Leeds LS2 9JT, UK

pysb@bath.ac.uk

**Abstract.** We have used high resolution Hall probe microscopy to image vortex-antivortex (V-AV) ‘molecules’ induced in superconducting Pb films by the stray fields from square arrays of ferromagnetic Co/Pt dots. We have directly observed spontaneous V-AV pairs and studied how they interact with added ‘free’ (anti)fluxons in an applied magnetic field. We observe a rich variety of subtle phenomena arising from competing symmetries in our system which can either drive added *antivortices* to join AV shells around nanomagnets or stabilise the translationally symmetric AV lattice between the dots. Added *vortices* annihilate AV shells, leading eventually to a stable ‘nulling’ state with no free fluxons, which should exhibit a strongly (field-)enhanced critical current. At higher densities we actually observe vortex shells around the magnets, stabilised by the asymmetric anti-pinning potential. Our experimental findings are in good agreement with Ginzburg-Landau calculations.

### 1. Introduction

Recent advances in nanofabrication and thin film growth technologies have made it possible to artificially engineer many of the properties of superconducting materials, for example through the introduction of ferromagnetic ‘dots’. Such superconductor-ferromagnet hybrid systems can be broadly divided into two classes; those with weak magnetic moments where the dots act as vortex pinning centres to enhance the superconducting critical current [1], and those with strong moments which lead to the spontaneous formation of vortex-antivortex (V-AV) pairs. The latter have been shown to exhibit magnetic field-induced superconductivity near the superconductor-normal state phase boundary due to the local compensation of the nanomagnet stray fields [2], but the situation deep within the superconducting state remains largely unexplored experimentally. In contrast there have been many theoretical investigations of superconducting films deposited on nanomagnet arrays using Ginzburg-Landau (GL) theory. Depending on its magnetic moment each magnet may generate one or more spontaneous vortex-antivortex (V-AV) pairs in the superconducting film. These either remain associated with individual magnets as V-AV ‘molecules’ in dilute arrays [3], or organize themselves into an ‘ionic’ crystal in dense arrays [4]. We report here the first direct images of spontaneous V-AV

structures captured using high resolution scanning Hall probe microscopy [5]. Our work yields key insights into how V-AV molecules transform into lattices and how they interact with (anti)fluxons introduced by external magnetic fields.

## 2. Experimental Methods

Our samples consist of square arrays of  $[\text{Co}(0.5\text{nm})/\text{Pt}(1\text{nm})]_{12}$  multilayer ferromagnetic disks, with uniaxial perpendicular anisotropy, covered with a type II superconducting Pb film (Fig. 1(a)). Four different diameter circular disks (522nm (A), 738nm (D), 808nm (B), 902nm (C)) with different magnetic moments have been patterned on the corners of a  $5\mu\text{m}\times 5\mu\text{m}$  square cell (Figs. 1(b),(c)) which was repeated periodically over a  $2\text{mm}\times 2\text{mm}$  area. Theoretical simulations indicated that these would generate in the range of 1 (dot A) to 5 (dot C) V-AV pairs [4]. Scanning Hall probe microscope (SHPM) images of magnetisation reversal in the disks at  $T=20\text{K}$  indicate a range of coercive fields spanning 700-1000Oe and magnetic saturation above  $H \cong 1000\text{Oe}$ . Magnetic switching of the disks is largely uncorrelated, but once magnetised they remain in a single domain state at  $H=0$  where they exhibit almost complete remanence. Hence, small applied fields ( $H < 100\text{Oe}$ ) can be applied to the superconducting film without any modification of the underlying magnetic ‘template’. Dc magnetron sputtering was used to coat the disks with a 20nm Ge layer (to suppress proximity effects) and the 80nm Pb film, followed by a 10nm Mo capping layer to prevent oxidation. Magnetisation measurements on an otherwise identical reference Pb film indicate that it is a type II superconductor with  $T_c = 6.68\text{K}$ ,  $\lambda_{\text{eff}}(5\text{K}) \cong 120\text{nm}$  and  $\xi(5\text{K}) \cong 50\text{nm}$ . Finally the sample was also coated with 20nm Ge and 50nm Au to enhance the stability of the SHPM when in tunnelling contact.

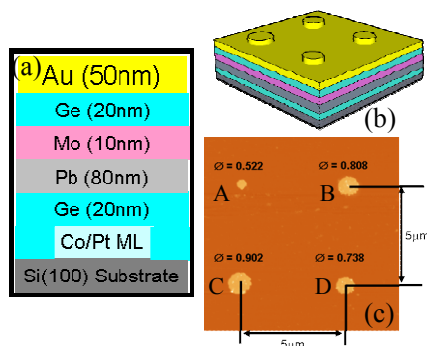


Figure 1 (a) Layer structure and (b) schematic diagram of the sample. (c) Atomic force microscope image of just the Co/Pt disks immediately after dry etching.

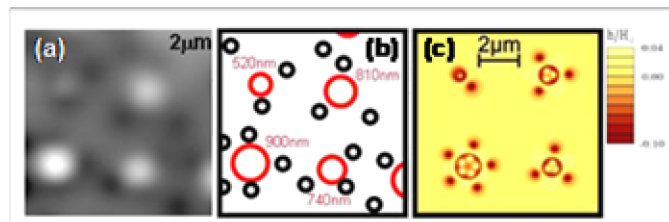


Figure 2 (a) SHPM image and (b) schematic depiction of spontaneous V-AV configurations at  $H_{\text{eff}} \cong 0$  and  $T = 5\text{K}$ . (c) Map of magnetic induction across the GL calculation under the same conditions.

High resolution SHPM has been used to visualise V-AV shell structures induced in the Pb film in the superconducting state. Our instrument is a modified commercial low temperature STM in which the usual tunnelling tip has been replaced by a microfabricated GaAs/AlGaAs heterostructure chip containing a  $\sim 500\text{nm}$  wire-width Hall cross (minimum detectable field  $\sim 1\mu\text{T}/\text{Hz}^{0.5}$ ) situated approximately  $5\mu\text{m}$  from the corner of a deep mesa etch. The latter had been coated with a thin Au layer to act as an integrated STM tip; this secondary sensor allows the sample surface to be found and the topography tracked while mapping the stray fields with the Hall sensor. A more detailed description of the instrument is given elsewhere [6].

Our experimental data have been compared directly with theoretical calculations based on solutions of the Ginzburg-Landau equations for our sample geometry assuming a coherence length  $\xi(0)=50\text{nm}$  and uniform magnetisation of the dots of  $M=750\text{G}$  (for more details of the approach we refer to [4]).

### 3. Experimental Results

Prior to magnetic imaging it was necessary to magnetise the dots to saturation ( $H > 3000\text{Oe}$ ) at low temperature. This resulted in the trapping of a small amount of magnetic flux in our superconducting solenoid, which acts in the opposite direction to the saturated dot magnetisation. We estimate that this background field (including the earth's magnetic field) is about  $-3.5\text{Oe}$ . The "effective" field values quoted here are defined as  $H_{\text{eff}} = H_a - 3.5\text{Oe}$ , where  $H_a$  is the externally applied field.

The SHPM images presented here were captured after field-cooling the sample from above  $T_c$  in the indicated applied field. Fig. 2(a) shows the first images of spontaneous V-AV 'shell' structures in our hybrid sample at  $H_{\text{eff}} = 0$  and  $T = 5\text{K}$ . A highly non-linear image grayscale has been used here to compensate for the fact that the amplitude of the (black) antivortices is typically only 10-20% of that of the (white) vortices trapped on the magnetic disks. As expected theoretically, the (black) AVs clearly order in shell-like structures around the magnetic dots, while (white) vortices remain confined above the dots. For clarity Fig. 2(b) shows a sketch of the precise AV locations as established from analysis of many line-scans across the SHPM image. The result of GL simulations of the local magnetic induction for the same sample geometry is shown in Fig. 2(c), and the predicted vorticity is in good agreement with that observed experimentally.

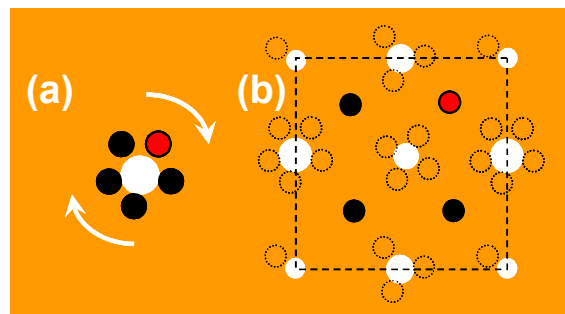


Figure 3 An excess antivortex (red dot) can experience a subtle competition between two types of ordered state; (a) an  $n$ -fold rotationally symmetric shell structure and (b) a translationally symmetric interstitial lattice.

The vorticity of V-AV shell structures can be tuned by applying a magnetic field to either add ( $H_{\text{eff}} < 0$ ) or annihilate ( $H_{\text{eff}} > 0$ ) antivortices. For negative applied fields we introduce free AVs into the spontaneous V-AV shell system. In this situation we find that there is a subtle competition between the  $n$ -fold rotational symmetry of the V-AV "molecules" and the translationally symmetric lattice of nanomagnets (Fig. 3). As the negative effective field is varied we sometimes observe spontaneous AVs which detach from their nanomagnet (effectively breaking a V-AV bond) to join the interstitial AV-lattice. At other field values we see the exact reverse of this and an AV in the interstitial lattice joins the AV shell around a magnetic dot, attracted by the 'positive' vortex core. At sufficiently negative effective fields all the V-AV molecules become net 'negative', i.e. they contain more antivortices than vortices (c.f. Fig. 4(a)).

For positive effective magnetic fields the behaviour of the V-AV structures is governed by the annihilation of AVs in shells by the externally added vortices. As the applied field is increased, each of the "molecules" progressively loses its negative AVs, and becomes more 'positively' charged. When all the AVs in a shell have been annihilated this leads to a fairly robust "nulling" state (c.f. Fig. 4(b)) that exists over a reasonably wide range of applied fields ( $\Delta H > 1\text{Oe}$ ). This 'locking' behaviour arises in this regime because additional vortices become trapped on the magnetic dots themselves

(increasing their vortex “charge”) because of the mutual attraction between a magnet and a vortex when their moments are parallel [7].

If the positive field is increased still further we start to see novel ordering phenomena of interstitial vortices. For  $H_{\text{eff}} = 4.5$  Oe a square interstitial vortex lattice is recovered, mirroring conventional matching phenomena (Fig. 4(c)). Surprisingly, at  $H_{\text{eff}} = 7.5$  Oe the presence of four different repulsive potentials propagating radially from the corners of the square cell, and strong interactions between interstitial vortices, results in their arrangement in shells (Fig. 4(d)). The same structures are found in GL simulations under identical conditions.

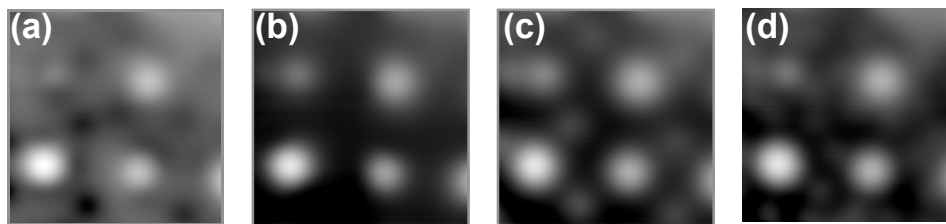


Figure 4 SHPM images of vortex-antivortex ‘shell’ structures at  $T = 5\text{K}$ . (a) Negatively charged V-AV ‘molecules’ at  $H_{\text{eff}} \cong -1\text{Oe}$ , (b) the “nulling” state at  $H_{\text{eff}} \cong 2\text{Oe}$ , (c) translationally ordered interstitial vortices at  $H_{\text{eff}} \cong 4.5$  Oe and (d) vortex shells at  $H_{\text{eff}} \cong 7.5\text{Oe}$ .

#### 4. Conclusions

In conclusion, we have made the first images of spontaneous V-AV shell structures induced in superconducting films by the stray fields of magnetic dots. We observe a variety of subtle phenomena which arise from competition between the  $n$ -fold rotational symmetry of the V-AV “molecules” and the translationally symmetric lattice of nanomagnets. All the features observed in our experiments are well reproduced in Ginzburg-Landau calculations for our sample geometry.

This work was supported in the UK by EPSRC grant No. GR/D034264/1 and PhD studentship GR/P02707/01. M.V.M. acknowledges support from EU Marie-Curie Intra-European program.

#### References

- [1] J.I. Martin et al., Phys. Rev. Lett. 79, 1929 (1997); D.J. Morgan et al., Phys. Rev. Lett. 80, 3614 (1998).
- [2] S.A. Wolf et al., Phys. Rev. B 25, 1990 (1982); H.W. Meul et al., Phys. Rev. Lett. 53, 497 (1984); M. Lange et al., Phys. Rev. Lett. 90, 197006 (2003).
- [3] M.V. Milosevic and F.M. Peeters, Phys. Rev. B 68, 024509 (2003).
- [4] M.V. Milosevic and F.M. Peeters, Phys. Rev. Lett. 93, 124509 (2004); D.J. Priour, Jr. and H.A. Fertig, Phys. Rev. Lett. 93, 057003 (2004).
- [5] J.S.Neal, M.V.Milosevic, S.J.Bending, A.Potenza, L. San Emeterio and C.H.Marrows, Phys. Rev. Lett. 99, 127001 (2007).
- [6] A.Oral, S.J.Bending and M.Henini, Appl. Phys. Lett. 69, 1324 (1996).
- [7] S. Erdin et al., Phys. Rev. B 66, 014414 (2002); M.V. Milosevic and F.M. Peeters, Phys. Rev. B 68, 094510 (2003); for review, see I. F. Lyuksyutov and V. L. Pokrovsky, Adv. Phys. 54, 67 (2005).